Egyptian Journal of Veterinary Sciences

https://ejvs.journals.ekb.eg/

Antimicrobial Susceptibility and Molecular Characterization of *Corynebacterium pseudotuberculosis* Isolates Recovered From Caseous Lymphadenitis in Sheep

Mohamed Bakr*[1], Mahmoud E. Hashad[1], Islam Gomaa[2] and Saad Attia[1]

[1] *Department of Microbiology and Immunology, Faculty of Veterinary Medicine, Cairo University, Giza, 12211, Egypt.*

[2] *Nanotechnology Research Centre (NTRC), The British University in Egypt, El-Shorouk City, Suez Desert Road, Cairo, 11837, Egypt.*

Abstract

Corynebacterium pseudotuberculosis is a well-recognized etiological agent responsible for caseous lymphadenitis (CLA) and ulcerative lymphangitis (UL) in small and large ruminants, respectively. This pathogen is frequently associated with poor therapeutic outcomes in animals. In the present study, 30 bacterial isolates, recovered from 300 lymph node and pus samples (10%), were identified as *Corynebacterium* spp. Molecular confirmation using 16S rRNA and *pld* gene PCR verified 11 of these isolates as *C. pseudotuberculosis*, while one isolate was identified as *C. jeikeium*, a first record from sheep in Egypt. The isolates were subjected to antimicrobial susceptibility and genotyping using enterobacterial repetitive intergenic consensus-polymerase chain reaction (ERIC-PCR). Cluster analysis classified the isolates into two major clusters: Cluster 1 (C1) represents *C. jeikeium*, and cluster 2 (C2) represents *C. pseudotuberculosis*. Cluster 2 was further subdivided into four subclusters (2A–2D), reflecting epidemiological linkages among livestock in Giza and Cairo governorates. Additionally, the antimicrobial potential of silver nanoparticles (AgNPs) and silver nitazoxanide-loaded nanoparticles (Ag-NPs/NTZ) was assessed against both *C. pseudotuberculosis* and *C. jeikeium*. The results revealed extensive multidrug resistance (MDR) among *C. pseudotuberculosis* and *C. jeikeium* isolates to several antibiotic classes. However, all *C. pseudotuberculosis* strains demonstrated 100% sensitivity to vancomycin, amoxicillin–clavulanic acid, gentamicin, and amikacin. These findings support the recommendation of these agents for effective control of CLA. Furthermore, silver nitazoxanide nanoparticles showed a promising in vitro effect against both *Corynebacterium* spp. recovered in this study and may represent a potential and novel adjunctive approach for managing *C. pseudotuberculosis* infections.

Keywords: *Corynebacterium*, ERIC-PCR, silver nanoparticles, silver nitazoxanide-loaded nanoparticles.

Introduction

Caseous lymphadenitis (CLA), caused by *Corynebacterium pseudotuberculosis*, is a chronic, infectious disease with significant veterinary and economic implications. It primarily affects sheep and goats but also impacts horses, cattle, and, in rare cases, humans [1-4]. This bacterium is Gram-positive, rod-shaped, pleomorphic, non-sporulated, non-capsulated, non-motile, facultative anaerobic, and facultative intracellular. It is characterized by a lipid-rich cell wall [5-7].

C. pseudotuberculosis's pathogenicity is driven primarily by phospholipase D (PLD) [8]. PLD increases vascular permeability, facilitating bacterial dissemination through lymphatic channels, while mycolic acids and iron acquisition systems, such as the fag operon, enhance intracellular survival by shielding the bacterium from lysosomal degradation and phagocytosis [9-11].

CLA is characterized by abscess formation in superficial and internal lymph nodes and, occasionally, visceral organs, often subclinical, complicating detection and control [12]. The disease is a major concern in small and large ruminant populations worldwide, causing substantial economic losses due to reduced wool, meat, and milk yields, premature culling, carcass condemnation, and trade restrictions [7, 13]. In Egypt, where CLA is endemic,

*Corresponding authors: Mohamed Bakr, E-mail: mbakr@cu.edu.eg, Tel.: +201110469346
(Received 18 August 2025, accepted 23 September 2025)
DOI: 10.21608/EJVS.2025.415210.3059

seroprevalence studies report infection rates ranging from 6.7% to 24.4% in sheep across various governorates [14-17].

Though rare, *C. pseudotuberculosis*'s zoonotic potential poses a public health risk, particularly for individuals with occupational exposure resulting in lymphadenitis or cutaneous abscesses mimicking tuberculosis or other gram-positive infections [6,18]. In addition, *C. pseudotuberculosis* was isolated from milk and milk products [19], posing a One-health threat. The global rise in antimicrobial resistance (AMR) further complicates CLA management, with Egyptian studies reporting resistance to antibiotics like penicillin, erythromycin, and tetracycline [20,21]. This highlights the critical need for comprehensive antimicrobial susceptibility testing to guide effective therapeutic approaches. There is an urgent need to use antibiotic replacements due to the growing antimicrobial resistance of bacteria [22]. Silver nanoparticles (AgNPs) are considered potent antimicrobial agents due to their broad-spectrum efficacy, low likelihood of inducing microbial resistance, and effective activity against biofilm formation [23]. Recently, nitazoxanide (NTZ)-loaded AgNPs display superior antibacterial efficacy to AgNPs alone [24]. Diagnosis of CLA is straightforward when superficial abscesses are visible but challenging for subclinical cases or internal abscesses, necessitating advanced methods like bacteriological culture, serological assays (e.g., ELISA), and molecular approaches [7,8]. Molecular tools, including polymerase chain reaction (PCR) targeting the *pld* gene, 16S rRNA gene sequencing, and Enterobacterial Repetitive Intergenic Consensus (ERIC)-PCR, enable precise identification and strain differentiation [25,26]. ERIC-PCR offers high-resolution fingerprinting, revealing shared clonal lineages across geographical zones and animal hosts, making it invaluable for epidemiological tracking during outbreaks of Gram-positive and Gram-negative bacteria [27, 28].

CLA control is often approached through antibiotic therapy guided by susceptibility testing, vaccination, and breeding for resistant breeds [29,7,8]. However, antimicrobial therapies are often limited by low diagnostic sensitivity and AMR, while vaccine adoption in regions like Egypt remains hindered by cost, limited awareness, and variable efficacy. Studies by [30,31] suggest that combining routine vaccination with biosecurity practices and molecular surveillance, such as ERIC-PCR, could significantly reduce CLA prevalence and economic losses.

Accordingly, this paper aimed to explore the incidence of CLA and the antimicrobial susceptibility profiles and molecular characterization of bacterial isolates recovered from clinical and postmortem samples. Meanwhile, the potential effect of silver nanoparticles and silver nitazoxanide nanoparticles on *C. pseudotuberculosis* and *C. jeikeium* was assessed.

Material and Methods

Sample collection, preparation, and bacterial isolation

A total of 300 samples (lymph nodes and pus) were collected aseptically from sheep, cattle, buffaloes, and camels. Suspected lymph nodes and internal samples were gathered from animals slaughtered in Bassatin and Monieb, major governmental slaughterhouses in Cairo and Giza, respectively. Clinical samples were obtained from animals recruited to veterinary units of Badrashin, Mazghona, Atifah, and Beni Suef. All specimens were transported promptly to the laboratory. Each lymph node was surface sterilised with absolute alcohol, briefly flamed, and then streaked onto blood agar supplemented with nalidixic acid (4 mg/L). Plates were incubated at 37°C for 48 hrs [32]. Presumptive colonies were examined by Gram staining.

Biochemical identification of the isolates

The isolates were then subjected to different biochemical tests, viz, catalase, urease, nitrate reduction, and gelatine liquefaction [33]. In addition, a non-pseudotuberculosis corynebacterium isolate was confirmed by API CORYNE 20 (BioMérieux, France).

Antimicrobial susceptibility testing of Corynebacterium pseudotuberculosis isolates

Based on the Kirby–Bauer (disc diffusion test) method, bacterial suspensions of PCR-confirmed isolates with a concentration matching the turbidity of McFarland tube No. 0.5 were subjected to antimicrobial susceptibility testing against 17 different antibacterial therapeutic agents on Mueller-Hinton-blood agar plates. The inhibition zone diameters were measured and judged according to breakpoints of the European Committee on Antimicrobial Susceptibility Testing (EUCAST, 2024) [34]. Isolates were classified as depicted in Tables 1 and 2 [35].

DNA extraction

The DNA was extracted from *C. pseudotuberculosis* isolates using a heat-based method in a total volume of 50 µl. Initially, the bacterial isolates were cultured onto blood agar plates for 48 hours at 37 °C. Bacterial colonies were harvested and washed 2 times in sterile, nuclease-free water. The bacterial pellet was suspended in 50 µl of sterile, nuclease-free water, and the DNA was released through thermal lysis, conducted at 100°C for 11 minutes, followed by cooling at 4°C for 4 minutes. The samples were centrifuged for 2 minutes at 14,000 g, and the supernatant containing the DNA was collected and frozen for further steps [36].

Molecular characterization of Corynebacterium pseudotuberculosis isolates

A PCR amplification targeting *Corynebacterium pseudotuberculosis* 16s rRNA gene [9] was conducted on the extracted DNA samples with modifications. Meanwhile, the *pld* gene PCR [36] was performed for confirmatory identification of *C. pseudotuberculosis*. In both types of PCR, the annealing temperature was modified to 52°C and 56°C, respectively. Primers and PCR cycling conditions are listed in the Table. 3. The reaction in both PCR assays comprised a final volume of 25 µl containing 2 µl of genomic DNA, 0.5 µM of each primer, 12.5 µl of PCR master mix (Genedirex), and 8.5 µl of nuclease-free water.

The amplification products were separated by electrophoresis in 1x TAE buffer and 1% agarose gels in the same type of buffer, stained with ethidium bromide. At the end of the run, bands were visualized using ultraviolet transillumination.

ERIC-PCR

Two trials were conducted to select the suitable conditions for *C. pseudotuberculosis* ERIC-PCR by using different primers, ERIC-1R (5′-ATGTAAGCTCCTGGGGATTCAC-3′), ERIC-2 (5′-AAGTAAGTGACTGGGGTGAGCG-3 ′), and the ERIC-1R + ERIC-2 primer pair [37], using different PCR conditions. The first trial conditions of thermal cycling were initiated with a denaturation step at 95°C for 5 min, followed by 30 cycles of denaturation at 95°C for 30 s, primer annealing at 52°C for 1 min, and elongation at 72°C for 2 min. The final extension step was performed at 72°C for 5 min as described by [25], On the contrary, the other trial conditions of thermal cycling were initiated with a denaturation step at 95°C for 12 minutes, followed by 45 cycles comprising denaturation at 95°C for 45 seconds, annealing at 35°C for 1 minute, and elongation at 70°C for 10 minutes. A final extension step was performed at 70°C for 20 minutes following the protocol previously described by [38].

The reaction mixture consisted of 6 µl of 5× HOT FIREPol® Blend Master Mix (Solis BioDyne, Estonia), 10 ng of genomic DNA, and 0.15 µM of each primer, adjusted to a final volume of 30 µl.

The amplified products were separated and visualized using the Bioanalyzer system (Agilent 2100) on a DNA 7500 gel. Banding patterns were evaluated using BioNumerics software version 7.5 (Applied Maths). The assay underwent in-house validation to assess reproducibility utilizing three technical and biological replicates.

Cluster analysis was conducted based on the Dice similarity coefficient, employing parameters of 0.5% optimization, 1% tolerance, and active zones defined within ±78%. Dendrograms were generated through the unweighted pair group method with arithmetic mean (UPGMA). Clustering of isolates was determined at an approximate similarity threshold of 80% [38]. The discriminatory power of the assay was assessed using the online Discriminatory Index (DI) calculator available at: http://insilico.ehu.es/mini_tools/discriminatory_power/index.php.

A dendrogram was constructed using GelJ software version 2.3, based on the polymorphic band patterns from ERIC-PCR, employing Jaccard coefficients and the unweighted pair group method [39].

Synthesis of Ag nanoparticles and nanocomposites

The synthesis followed a reported procedure with minor modifications [40]. Briefly, 1.0 g $AgNO_3$ was dissolved in an appropriate solvent at 70 °C under vigorous magnetic stirring for 2 h until a clear solution was obtained. The pH was then raised to 11 by dropwise addition of 1 M KOH, at which point turbidity indicated the onset of nucleation. After 2 h of stirring, the reaction mixture was probe-sonicated (pulsed mode, 20 kHz) for 30 min to promote controlled nucleation and growth. The product was recovered by centrifugation and washed three times with Milli-Q water (9,000 rpm, ~10 min per wash). Finally, the collected material was dried in a vacuum oven at 200 °C for 12 h to yield the grey AgNP powder. Thirty milligrams of Ag NP powder were accurately weighed and combined with 70 mg of nitazoxanide using a mortar and pestle. The powder blends were then suspended in Milli-Q water adjusted to pH 5.5 and sonicated in a bath sonicator for 5 min to get intimate contact between the nanoparticles and the NTZ. After centrifugation (9,000 rpm, 10 min), the recovered Ag-NP/NTZ composites were dried in an oven at 70 °C for 6 h.

Assessment of the in vitro antimicrobial efficacy of silver nanoparticles and silver-nitazoxanide nanoparticles using the well diffusion method

Bacterial suspensions of PCR-confirmed isolates, with a concentration corresponding to the turbidity of McFarland tube No. 0.5, were subjected to antimicrobial susceptibility testing against 1%, 2.5%, and 5% (w/v) in sterile distilled water of both AgNPs and AgNPs/NTZ [41] on Mueller-Hinton blood agar using the well diffusion method. Positive and negative controls were represented by vancomycin and sterile distilled water, respectively. NTZ was not used as a control by itself, as it is considered a scaffold rather than an antibacterial agent alone [40].

Results

Gross lesions of CLA in sheep lymph nodes were observed as caseated and suppurative materials with an onion-like appearance (Fig. 1). Of 300 samples examined in this study, *Corynebacterium spp.* were recovered from 30 (10%). However, only 11 isolates were confirmed to be *C. pseudotuberculosis* via PCR

assays targeting the species-specific 16S rRNA and the *pld* genes (Fig.s 2 and 3). In addition, a *C. jeikeium* isolate was obtained from a sheep lymph node.

The identification of *C. pseudotuberculosis* isolates was conducted through a combination of microscopic, cultural, and biochemical methods. Microscopically, the isolates appeared as Gram-positive coccobacilli arranged in V, L, and palisade forms. On sheep blood agar, the colonies exhibited distinctive morphological characteristics, appearing round, whitish to greyish, shiny, and slightly mucoid, typically surrounded by a narrow zone of β-haemolysis with a crackling sound when subjected to direct flame.

Biochemically, the isolates were catalase- and urease-positive while negative for gelatin liquefaction. Isolates from sheep were nitrate reductase negative, while isolates from cows were positive. *C. jeikeium* was confirmed biochemically using API CORYNE 20, resulting in positive results for catalase, pyrazinamidase, alkaline phosphatase, glucose, and ribose fermentation. Meanwhile, the isolate was negative for nitrate reductase, urease, gelatin liquefaction, esculin hydrolysis, pyrrolidonyl arylamidase, β-glucuronidase, β-galactosidase, α-glucosidase, β-N-Acetyl-Glucosaminidase, and fermentation of xylose, mannitol, maltose, lactose, sucrose, and glycogen [42].

The antimicrobial susceptibility testing of *C. Pseudotuberculosis* isolates showed variable susceptibility to various classes of antibacterial agents. It was found that 100% of the isolates showed sensitivity for vancomycin, gentamycin, amikacin, rifampin, amoxicillin-clavulanate, and chloramphenicol. Sensitivity for tetracycline, ciprofloxacin, and azithromycin was conferred by 10/11 (90.9%), 10/11 (90.9%), and 8/11 (72.7%) of the isolates, respectively. On the other hand, 100% of the isolates conferred resistance to fosfomycin, nitrofurantoin, and nalidixic acid. In addition, cefotaxime, ampicillin, and trimethoprim-sulfamethoxazole demonstrated low efficacy, with resistance detected in 10/11 (90.9%), 7/11 (63.6%), and 7/11 (63.6%) of the isolates, respectively. Intermediate resistance was noted against erythromycin and streptomycin by 6/11 (54.5%) and 4/11 (36.3%) of the isolates, respectively (Tables 1 and 2).

Regarding the *C. jeikeium* isolate, it was sensitive to vancomycin, tetracycline, ciprofloxacin, ampicillin, rifampin, erythromycin, trimethoprim-sulfamethoxazole, streptomycin, gentamycin, amikacin, azithromycin, and amoxicillin-clavulanic acid while resistant to cefotaxime, chloramphenicol, nalidixic acid, fosfomycin, and nitrofurantoin (Tables 1 and 2).

Nanocomposite Characterization

Fig. 4 summarizes the structural and morphological characterization of the as-synthesized silver nanoparticles (Ag NPs) and the Ag-nitazoxanide (Ag-NPs/NTZ) nanocomposite. The X-ray diffraction (XRD) pattern of the dried AgNPs (Fig. 4a) displays sharp, well-defined reflections at 2θ = 38.103°, 44.311°, 64.455°, 77.404°, and 81.521°, which correspond to d-spacings of 2.3598, 2.0435, 1.4446, 1.2319, and 1.1798 Å, respectively. These signals match previously reported diffraction features for crystalline nitazoxanide (NTZ) and demonstrate the coexistence of intact NTZ domains and fcc silver in the composite, supporting successful incorporation of Ag NPs into the NTZ matrix.

Morphological examination by field-emission scanning electron microscopy (FE-SEM) further corroborates the XRD findings. Images of the isolated Ag NPs at 4,000× and 8,000× magnification (Fig. 4c–d) reveal predominantly plate and discrete nanoparticles with an average particle size of ≈70 nm and a tendency to form compact aggregates, consistent with high surface energy and partial sintering during drying. In the Ag-NPs/NTZ composite (Fig. 4e–f), the silver nanoparticles are observed adhered to and partially embedded within the plate-like NTZ crystallites, including accumulation at plate termini.

The antimicrobial effect of silver nanoparticles (AgNPs) and nitazoxanide-loaded silver nanoparticles (AgNPs/NTZ) was evaluated against *Corynebacterium pseudotuberculosis* and *Corynebacterium jeikeium*. AgNPs/NTZ exhibited significantly enhanced activity compared to AgNPs alone. (Fig. 5) A direct proportional relationship was noticed between the concentration of both types of AgNPs and the inhibition zone diameter excreted against *C. pseudotuberculosis* and *C. jeikeium* (Fig. 5 & Table 4). The inhibition zone diameters were 7.5, 8.5, and 10.27 mm with the concentrations of 1%, 2.5% and 5% of AgNPs, respectively, against *C. pseudotuberculosis,* while the inhibition zones were 8.5, 9, and 10.5 mm with the same concentrations, respectively, against *C. jeikeium.* On the other hand, the inhibition zone diameters were 10.71, 12.29, and 15.64 mm with the concentrations of 1%, 2.5% and 5% of AgNPs/NTZ, respectively, against *C. pseudotuberculosis,* while the inhibition zones were 16, 17, and 17 mm with the same concentrations, respectively, against *C. jeikeium.*

ERIC-PCR on corynebacterial genomic DNA

The ERIC-PCR using the ERIC 2 primer with the conditions described by [38] showed the best results concerning the bands' number and sharpness, consequently allowing more genetic diversity between isolates.

ERIC-PCR of 11 *C. pseudotuberculosis* isolates and one *C. jeikeium* isolate revealed distinct genetic relationships, forming two major clusters at ~72% similarity. Cluster 1 included only the *C. jeikeium* isolate. Cluster 2 comprised all 11 C. pseudotuberculosis isolates and was further divided into four subclusters (2A–2D) at ~77% similarity, as shown in Fig. 6.

Discussion

Caseous lymphadenitis (CLA) is a suppurative disease that affects small ruminants and is clinically characterized by the formation of abscesses in superficial and internal lymph nodes. The disease results in significant production losses in wool, meat, and milk yields, increased culling rates, and condemnation of carcasses [25,43].

In the current study, corynebacterium isolates were recovered from 10% of pus and lymph node samples, which matches the findings of previous studies in Egypt [14,15,16,17]. It was reported that CLA has been endemic in Egypt, with seroprevalence rates ranging from 6.7% to 24.4% in sheep across various governorates. In addition, [44] reported that *C. pseudotuberculosis* was confirmed using PCR in 10% of sheep lymph nodes.

Of 30 Corynebacterium isolates identified on morphological and biochemical bases, 11 were *C. pseudotuberculosis* as confirmed by PCR assays targeting the 16S rRNA and *pld* genes of the species. The relatively low incidence recorded in this study could be attributed to the limited geographic area covered in the study, as well as the vaccination followed by the owners against CLA. Even though epidemiological elucidation was not a target in this study, the obtained isolates were sufficient for antimicrobial and molecular studies.

A *C. jeikeium* isolate was recovered from sheep lymph node and confirmed using the API CORYNE 20 system. This finding was astonishing as the lesion, from which it was isolated, was a typical CLA lesion. Based on what we have of the literature, this is the first record of *C. jeikeium* isolation from sheep in Egypt. However, [45] reported its isolation from camel lymph nodes. Interestingly, [46] recovered *C. jeikeium* from keratitis in a human patient, highlighting its zoonotic and one-health impact.

In this study, antimicrobial susceptibility profiles for 11 *Corynebacterium pseudotuberculosis* and 1 *C. jeikeium* isolates revealed variable responses across 17 antibacterial agents. The *C. pseudotuberculosis* isolates exhibited complete susceptibility (100%) to vancomycin, gentamycin, amikacin, amoxicillin-clavulanate, and chloramphenicol. These findings match those of [47], who reported that all corynebacterium isolates were fully susceptible to a wide range of antibiotics. The results are also similar to the findings of [48] concerning chloramphenicol.

In contrast, high resistance rates were conferred against fosfomycin, nitrofurantoin, and nalidixic acid, as all isolates showed uniform resistance to the three agents (100%), which is matched with the findings of [48] who reported 100% resistance of *C. pseudotuberculosis* to nitrofurantoin. Similarly, cefotaxime and trimethoprim-sulfamethoxazole faced high resistance. In contrast to our results, [47] recorded strong susceptibility to cephalosporin. However, our results are compatible with those of [20] regarding trimethoprim-sulfamethoxazole.

In this study, intermediate resistance was noted for erythromycin and streptomycin, similar to what was reported by [20,44]. Our data also show variable susceptibility to azithromycin, with 2 isolates showing intermediate responses, potentially indicating evolving resistance.

Regarding ampicillin, 7 *C. pseudotuberculosis* isolates displayed resistance, while one isolate was intermediately sensitive. Similar findings were reported by [49,44], who reported strong resistance of *C. pseudotuberculosis* against ampicillin.

Tetracycline and ciprofloxacin displayed high efficacy against most isolates, confirming the results recorded by [47,49] regarding tetracycline and quinolones, respectively.

In this investigation, it was surprisingly found that the lone obtained *C. jeikeium* isolate showed a multi-drug resistance (MDR) as it conferred resistance to five antimicrobial agents belonging to five different classes (cefotaxime, fosfomycin, nalidixic acid, nitrofurantoin, and chloramphenicol). In previous studies, [50,51,52] indicated that of the true *Corynebacterium* species, *C. jeikeium* had multiple antibiotic resistance. Testing our isolates against Fosfomycin, nalidixic acid, and nitrofurantoin was a confirmatory testing, as *C. pseudotuberculosis* is known for its resistance to the three agents [48].

As the results of the antimicrobial sensitivity of corynebacterium isolates of this study were not promising for therapeutic application, it was of significance to look for alternatives.

Concerning the physicochemical characteristics of nanoparticles prepared in our study, the reflections obtained with the prepared nanoparticles were indexed to the (111), (200), (220), (311) and (222) planes of face-centered cubic (fcc) silver (space group Fm-3m), in good agreement with the ICDD reference pattern (01-080-4432) [40] and confirm the highly crystalline nature of the synthesized Ag NPs. The XRD trace of the Ag-NPs/NTZ nanocomposite (Fig. 4b) contains the characteristic Ag reflections together with additional low-angle peaks (marked with asterisks) at $2\theta = 5.2808°$, 13.2106°, 15.8698°, 17.6981°, 21.2098°, and 23.1297°, corresponding to d-spacings of 16.711, 6.701, 5.583, 5.001, 4.175, and

3.842 Å, respectively. The close interfacial contact and the even distribution of nanoscale Ag on the NTZ surfaces indicate good mixing and effective physical integration of the composite components, which is expected to influence the composite's interfacial properties and functional performance. [40].

Nano-formulated materials have been extensively assayed for their antimicrobial efficacy. Silver nanoparticles (AgNPs) in earlier studies demonstrated the efficacy of metallic nanoparticles against *C. pseudotuberculosis*. Notably, [23] reported that biogenic AgNPs showed strong activity against both planktonic and biofilm forms of *C. pseudotuberculosis*, with notable reductions in metabolic activity and viable cell counts. [53] also reported that the efficacy of AgNP-based ointment as a post-surgical treatment for caseous lymphadenitis (CL) appeared to be a promising approach, promoting faster wound healing, reducing microbial contamination, and showing no observable toxic effects.

Combining nitazoxanide nanoparticles, a broad-spectrum antiprotozoal and antibacterial agent, with AgNPs significantly improved efficacy, supporting the hypothesis of synergistic interaction. Nitazoxanide interferes with anaerobic metabolism and has been shown to enhance silver ion release and membrane disruption when combined with metallic carriers [24]. No previous studies discussed the effect of NTZ on *Corynebacterium* spp. These results emphasize the potential of AgNPs/NTZ in combating multidrug-resistant pathogens and the importance of molecular surveillance in managing corynebacterium infections.

Genotypically, *C. jeikeium* and *C. pseudotuberculosis* were categorized into two distinct clusters based on the ERIC-PCR dendrogram. Meanwhile, the distinct antimicrobial resistance phenotype further validates this classification and supports ERIC-PCR as a powerful epidemiological and genotypic typing tool. In this regard, the discriminatory power of ERIC-PCR at the species level for corynebacteria has been documented for the first time in this study. According to what we have of the literature, no previous studies have tried to assess the genetic relationship between *C. jeikeium* and *C. pseudotuberculosis*.

In this study, the ERIC 2 primer with the conditions described by [38] allowed more genetic diversity between isolates. An increased number and sharpness of bands were obtained with the ERIC 2 primer. This could be attributed to the longer time, which gives a chance for the primer to work well.

Based on ERIC PCR, Cluster 2 that comprised *C. pseudotuberculosis* isolates has been subdivided into four subclusters (A-D), each showing specific genetic groupings and corresponding resistance trends as follow: subcluster 2A (ovine isolates: 66, 125, 135) at ~90% similarity, These isolates, despite originating from different locations (Bassatin and Monieb), exhibited close genetic similarity and shared resistance to five drug classes (ampicillin, cefotaxime, fosfomycin, nalidixic acid, and nitrofurantoin), suggesting a clonal lineage possibly driven by flock movement, shared infection sources, or uncontrolled animal movement [25,38]. Subclusters 2B and 2C (isolates 212, 224) at ~77.5% similarity were derived from a sheep and a cow in Bassatin, respectively. These isolates showed broad-spectrum MDR (resistance to 6 classes: ampicillin, cefotaxime, fosfomycin, nalidixic acid, nitrofurantoin, and erythromycin), indicating a close genetic relationship between species-specific corynebacteria or environmental persistence in mixed-species housing. Subcluster 2D comprised isolates 172, 310, 75, N, 205, 225 at ~82% similarity. Although this group showed greater genetic and phenotypic variability between isolates N, 225, and 205, there was a strong genetic similarity between isolates 172 and 310 at ~92% similarity. These were sheep isolates from different localities (Monieb and Bassatin), evidencing once more the uncontrolled animal movement that could be a potential route of disease transmission. The subcluster 2D isolates surprisingly showed extensive MDR as they resist 10 drug classes (ampicillin, erythromycin, fosfomycin, nalidixic acid, nitrofurantoin, streptomycin, trimethoprim-sulfamethoxazole, erythromycin, tetracycline, and ciprofloxacin). Isolates 225 and 205 at 82% similarity were originating from sheep and cow, indicating a close genetic relationship despite being different nitrate reduction biotypes. Although both isolates were resistant to 3 antibiotic classes (fosfomycin, nalidixic acid, and nitrofurantoin), isolate 225 was resistant to 8 classes, the most extensive pattern observed. This diversity may reflect multiple infection sources or evolving resistance within this lineage.

Mapping resistance profiles onto the dendrogram revealed a strong correlation between genotypic clusters and antimicrobial susceptibility. Subclusters 2A–2C showed consistent resistance trends, while 2D exhibited more phenotypic divergence. The presence of both intra- and interspecies clustering (e.g., cow and sheep in the same subclusters) further highlights potential inter-species transmission routes or shared environmental reservoirs. These findings are in line with previous ERIC-PCR studies, such as [38,54], which demonstrated ERIC-PCR's high discriminatory index (HGDI ~0.92–0.94) and its capacity to detect biovar or geography-linked clusters and resistance-associated patterns of *C. pseudotuberculosis*. ERIC PCR is more convenient and easier to perform if compared to Pulsed-field gel electrophoresis (PFGE) or nucleotide sequence analysis. Moreover, PFGE provides biovar-level

resolution but is less effective in differentiating closely related Ovis strains [55].

Conclusion

Corynebacterium pseudotuberculosis and *C. jeikeium* recovered in this study showed varying antibiotic resistance patterns to several antibiotic classes, with consistent multidrug resistance. This was particularly noted in *C. jeikeium*. Effective antibiotics such as vancomycin, amoxicillin-clavulanate, gentamicin, amikacin, ciprofloxacin, and tetracycline are recommended for CLA control. Additionally, nitazoxanide-loaded silver nanoparticles demonstrated enhanced antimicrobial activity, offering a promising alternative against multidrug-resistant strains. Continued surveillance and biosecurity are essential for effective disease management. ERIC-PCR revealed genetic diversity and potential transmission between species and locations. This study may be of significance for guiding control programs of CLA in small ruminants.

Acknowledgments

Not applicable.

Funding statement

This study didn't receive any funding support

Declaration of Conflict of Interest

The authors declare that there is no conflict of interest.

Ethical of approval

Not applicable.

TABLE 1. Antimicrobial sensitivity of C. *pseudotuberculosis* and *C. jeikeium* isolates

	C. pseudotuberculosis			% Resistance (R)	*C. jeikeium*
	S (n/11)	I (n/11)	R (n/11)		
Vancomycin	(11/11)	(0/11)	(0/11)	0	S
Tetracycline	(10/11)	(0/11)	(1/11)	8.3	S
Ciprofloxacin	(10/11)	(0/11)	(1/11)	8.3	S
Cefotaxime	(2/11)	(0/11)	(9/11)	83.3	R
Ampicillin	(3/11)	(1/11)	(7/11)	58.3	S
Rifampin	(11/11)	(0/11)	(0/11)	0	S
Erythromycin	(6/11)	(1/11)	(4/11)	33.3	S
Trimethoprim-sulfamethoxazole	(6/11)	(0/11)	(5/11)	41.7	S
Streptomycin	(6/11)	(0/11)	(5/11)	41.7	S
Gentamycin	(11/11)	(0/11)	(0/11)	0	S
Fosfomycin	(0/11)	(0/11)	(11/11)	100	R
Nitrofurantoin	(0/11)	(0/11)	(11/11)	100	R
Nalidixic acid	(0/11)	(0/11)	(11/11)	100	R
Amikacin	(11/11)	(0/11)	(0/11)	0	S
Azithromycin	(8/11)	(2/11)	(1/11)	8.3	S
Amoxicillin-clavulanate	(11/11)	(0/11)	(0/11)	0	S
Chloramphenicol	(11/11)	(0/11)	(0/11)	0	R

* S: sensitive; I: intermediately sensitive, R: resistant.

TABLE 2. The antimicrobial resistance patterns of *C. Pseudotuberculosis* and *C. jeikeium* isolates to antimicrobial classes

Number of Examined Isolates	Number of resisted classes
2	5 classes
2	7 classes
2	4 classes
1	5 classes
1	8 classes
1	3 classes
1	6 classes
1	7 classes
1	8 classes

TABLE 3. Primer sequences, target genes, amplicon sizes, and cycling conditions of PCR assays

Target Gene Primary	Primers Sequences (5'-3')	Amplified Segment (bp)	Primary Denaturation	Amplification (35 Cycles)			Final Extension
				Secondary Denaturation	Annealing	Extension	
***C.* Pseudotuberculosis 16S rRNA**	F-ACCGCACTTT AGTGTGTGTG R-TCTCTACGC CGATCTTGTAT	812	94 °C 3 min	94 °C 30 Sec	52 °C 45 Sec	72 °C 1 min	72 °C 10 min
Target Gene Primary	**Primers Sequences**	**Amplified Segment (bp)**	**Primary Denaturation**	**Amplification (40 Cycles)**			**Final Extension**
				Secondary Denaturation	**Annealing**	**Extension**	
***Pld* gene**	F-ATGAGGGAGAAAG TTGTTTTA R-TCACCACGGGTTA TCCGC	924	94 °C 5 min	94 °C 40 sec	56 °C 40 sec	72 °C 40 sec	72 °C 10 min

TABLE 4. Mean inhibition zone diameters ± SD in (mm) exerted by silver nanoparticles singly or combined with nitazoxanide

Agent	Concentration	*C. pseudotuberculosis*	*C. jeikeium*
Vancomycin	30 µg/disc	29.36 ± 4.74	34
AgNPs	1%	7.5 ± 0.5	8.5
	2.5%	8.5 ± 0.5	9
	5%	10.27 ± 1.62	10.5
Ag-NPs/NTZ	1%	10.71 ± 1.80	16
	2.5%	12.29 ± 2.21	17
	5%	15.64 ± 4.18	17

Fig.. 1. The characteristic CLA lesions in sheep lymph nodes: caseation and onion-like appearance.

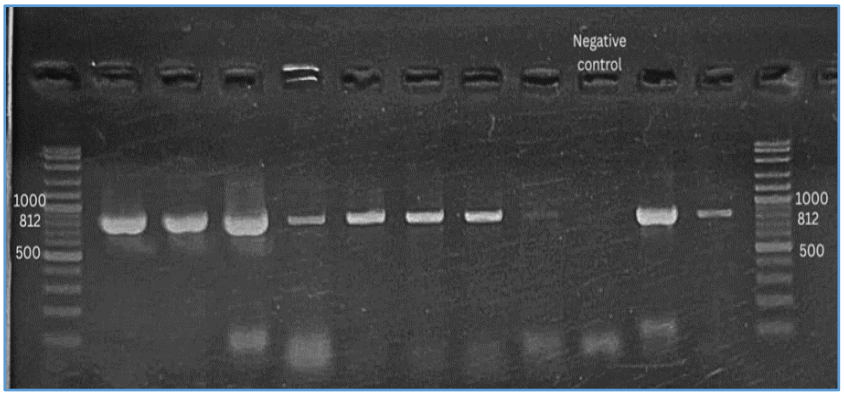

Fig. 2. Agarose gel electrophoresis showing amplicons of 812 bp of the 16S rRNA in *C. pseudotuberculosis* isolates.

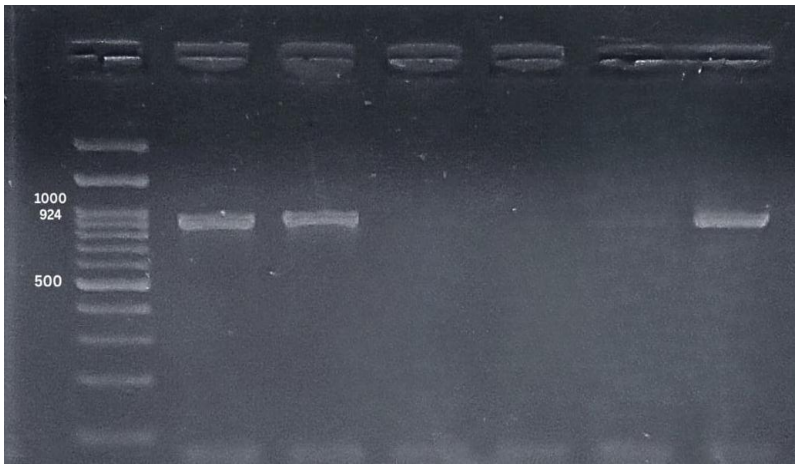

Fig. 3. Agarose gel electrophoresis showing the amplicon size (924 bp) of *pld* gene of *C. pseudotuberculosis* isolates

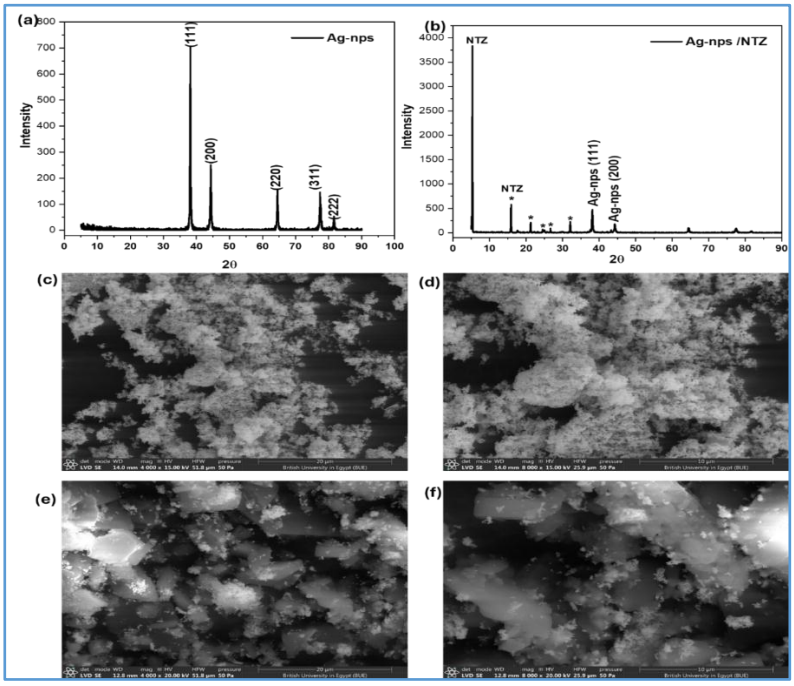

Fig. 4. Multimodal characterization of Ag NPs and the Ag–NTZ nanocomposite. (a, b) X-ray diffraction patterns of pristine Ag NPs and the Ag-NPs/NTZ composite, respectively. (c, d) FE-SEM micrographs of isolated Ag NPs at 4,000× and 8,000× magnification. (e, f) FE-SEM micrographs of the Ag-NPs/NTZ nanocomposite at 4,000× and 8,000× magnification, respectively.

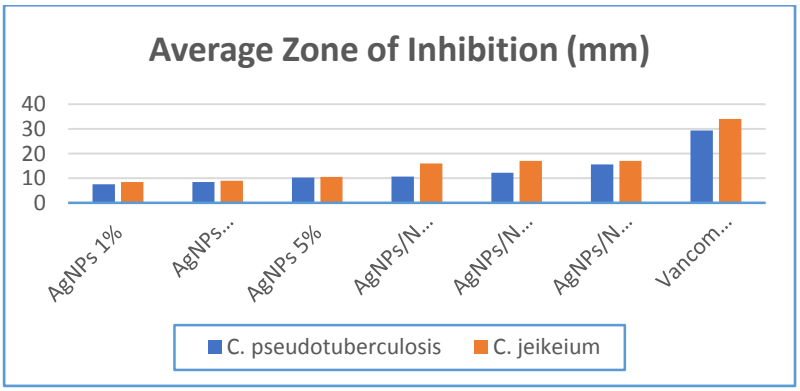

Fig. 5. A graphic representation of the mean zone of inhibition in mm of AgNPs (silver nanoparticles), AgNPs/NTZ (silver nanoparticles-loaded nitazoxanide), and Vancomycin (control positive) against *C. jeikeium* (orange bar) and *C. pseudotuberculosis* (blue bar).

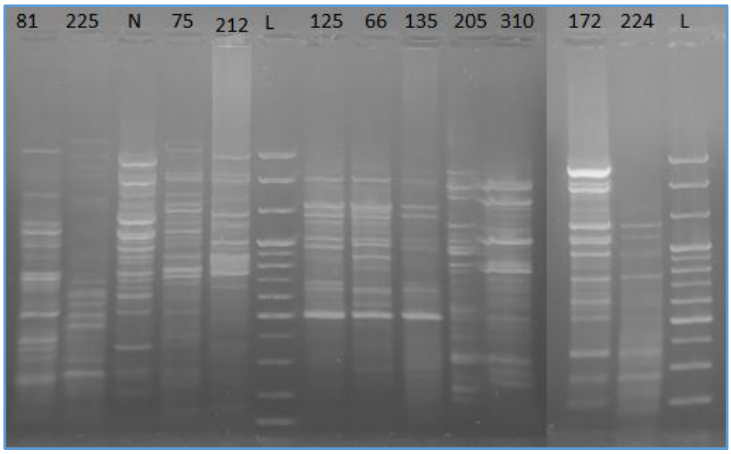

Fig. 6. Agarose gel electrophoresis of ERIC-PCR products, 81 (*C. jeikeium*, sheep, Monieb), 135, 125, 212, 172, N, 205 (*C. pseudotuberculosis*, sheep, Bassatin), 66, 75,310 (*C. pseudotuberculosis*, sheep, Monieb), 224, 225 (*C. pseudotuberculosis*, cow, Bassatin), L (DNA ladder).

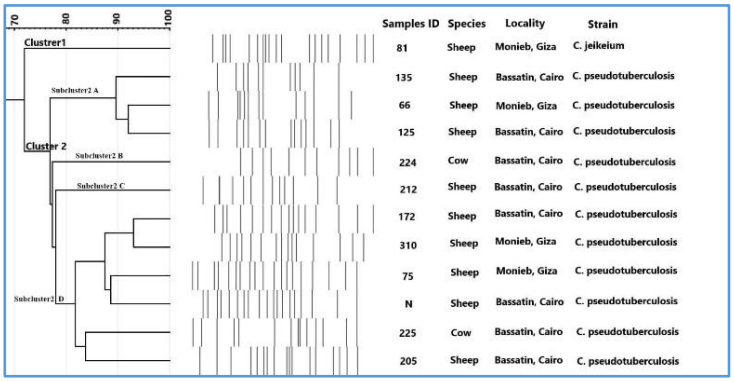

Fig. 7. An ERIC-PCR-based dendrogram illustrating the genetic relatedness of Corynebacterium isolates, 81 (*C. jeikeium*, sheep, Monieb), 135, 125, 212, 172, N, 205 (*C. pseudotuberculosis*, sheep, Bassatin), 66, 75,310 (*C. pseudotuberculosis*, sheep, Monieb), 224, 225 (*C. pseudotuberculosis*, cow, Bassatin).

References

1. Sellon, D. C., Spier, S. J., Whitcomb, M. B., Arguedas, M. G., Long, M. T., Oaks, J. L. and Hines, M. T. 'Chapter 45 - Miscellaneous Bacterial Infections', in Sellon, D. C. and Long, M. T. (eds), Equine Infectious Diseases (Second Edition), St. Louis, W.B. Saunders, 373-392.e6 (2014) DOI: https://doi.org/10.1016/B978-1-4557-0891-8.00045-2.
2. Williamson, L. H. Caseous lymphadenitis in small ruminants, The Veterinary clinics of North America. *Food Animal Practice*, **17** (2),5 (2001). DOI: 10.1016/S0749-0720(15)30033-5.
3. Connor, K. M., Fontaine, M. C., Rudge, K., Baird, G. J. and Donache, W. Molecular genotyping of multinational ovine and caprine *Corynebacterium pseudotuberculosis* isolates using pulsed-field gel electrophoresis, *Veterinary Research*, **38** (4), 613–623 (2007). DOI: 10.1051/vetres:2007013.
4. Join-Lambert, O. F., Ouache, M., Canioni, D., Beretti, J. L., Blanche, S., Berche, P. and Kayal, S. *Corynebacterium pseudotuberculosis* necrotizing lymphadenitis in a twelve-year-old patient. *The Pediatric Infectious Disease Journal*, **25**(9), 848–851 (2006).https://doi.org/10.1097/01.inf.0000234071.93044.77
5. Barksdale, L. *Corynebacterium diphtheriae* and Its Relatives, *BACTERIOLOGICAL REVIEWS*, **34** (4), (1970). DOI: https://journals.asm.org/journal/br.
6. Bastos, B. L., Portela, R. D., Dorella, F. A., Ribeiro, D., Seyffert, N., Castro, T. L. D. P. and Azevedo, V. *Corynebacterium pseudotuberculosis*: immunological responses in animal models and zoonotic potential. *J Clin Cell Immunol.*, **1** (S4), 10-4172 (2012). DOI: 10.4172/2155-9899.s4-005.
7. Baird, G. J. and Fontaine, M. C. *Corynebacterium pseudotuberculosis* and its Role in Ovine Caseous Lymphadenitis, *Journal of Comparative Pathology*, **137**, (4), (2007). DOI: 10.1016/j.jcpa.2007.07.002.
8. Dorella, F., Gustavo, L., Pacheco, C., Oliveira, S., Miyoshi, A., Azevedo, V., Dorella, F. A. and Oliveira, S. C. *Corynebacterium pseudotuberculosis*: microbiology, biochemical properties, pathogenesis and molecular studies of virulence, *Veterinary Research*, **37** (2), 201–218 (2006). DOI: 10.1051/vetres:2005056ï.

9. Pacheco, L. G. C., Pena, R. R., Castro, T. L. P., Dorella, F. A., Bahia, R. C., Carminati, R., Frota, M. N. L., Oliveira, S. C., Meyer, R., Alves, F. S. F., Miyoshi, A. and Azevedo, V. Multiplex PCR assay for identification of *Corynebacterium pseudotuberculosis* from pure cultures and for rapid detection of this pathogen in clinical samples, *Journal of Medical Microbiology*, **56** (4), 480–486 (2007). DOI: 10.1099/jmm.0.46997-0.

10. Billington, S. J., Esmay, P. A., Songer, J. G., & Jost, B. H. Identification and role in virulence of putative iron acquisition genes from *Corynebacterium pseudotuberculosis*. *FEMS Microbiology Letters*, **208**(1), 41–45 (2002). https://doi.org/10.1111/j.1574-6968.2002.tb11058.x

11. Odhah, M. N., Jesse, F. F. A., Bura, P., Chung, E. L. T., Nor, N. F. M., Norsidin, J. M. and Mohd-Lila, M. A. Current Review on Mycolic Acid Immunogen of *Corynebacterium pseudotuberculosis*. *Journal of Advanced Veterinary Research*, **12**(2), 177-186 (2022).

12. Khalafalla, A. I. and Hussein, M. F. Infectious diseases of dromedary camels. Cham, Switzerland: Springer International Publishing (2021).

13. De Jesus Sousa, T., Jaiswal, A. K., Hurtado, R. E., De Oliveira Tosta, S. F., De Castro Soares, S., Gomide, A. C. P., Alcantara, L. C. J., Barh, D., Azevedo, V. and Tiwari, S. Pan-genomics of veterinary pathogens and its applications', in Pan-genomics: Applications, Challenges, and Future Prospects, Elsevier, *Academic Press*, 101–119 (2020). DOI: 10.1016/B978-0-12-817076-2.00005-6.

14. Sayed, A.M., Abd El-fattah, A.M., Manna, A.M. and Sayed, A.M. Caseous lymphadenitis of sheep at Assiut governorate: disease prevalence, lesion, distribution, and bacteriological, *Assiut Veterinary Medical Journal*, **33** (65), 88–92 (1994).

15. Selim, A. M., Atwa, S. M., El Gedawy, A. A., Hegazy, Y. M., Rizk, M. A. and Younis, E. E. Risk factors associated with the seroprevalence of caseous lymphadenitis in sheep. *Comparative Clinical Pathology*, **30**(2), 285-291 (2021). DOI: 10.1007/s00580-021-03198-0/Published.

16. Burmayan, A. and Brundage, C. M. Caseous lymphadenitis outbreak in a small ruminant herd, *Open Veterinary Journal, Faculty of Veterinary Medicine, University of Tripoli,* **11** (4), 530–534 (2021). DOI: 10.5455/OVJ.2021.v11.i4.2.

17. Rizk, A. M., Abd El-Tawab, A. A., Afifi, S. E. and Mohamed, S. R. *Corynebacterium pseudotuberculosis* infection in small ruminant and molecular study of virulence and resistance genes in Beni-Suef Governorate. *Benha Veterinary Medical Journal*, **37**(1), 122-127 (2019).

18. Peel, M. M., Palmer, G. G., Stacpoole, A. M. and Kerr, T. G. Human lymphadenitis due to *Corynebacterium pseudotuberculosis*: report of ten cases from Australia and review. *Clinical Infectious Diseases*, **24**(2), 185-191 (1997). http://cid.oxfordjournals.org/.

19. Langova, D., Slana, I., Okunkova, J., Moravkova, M., Florianova, M. and Markova, J. First Evidence of the Presence of the Causative Agent of Caseous Lymphadenitis—*Corynebacterium pseudotuberculosis* in Dairy Products Produced from the Milk of Small Ruminants, *Pathogens*, MDPI, **11** (12), (2022). DOI: 10.3390/pathogens11121425.

20. El Damaty, H. M., El-Demerdash, A. S., Abd El-Aziz, N. K., Yousef, S. G., Hefny, A. A., Abo Remela, E. M., Shaker, A. and Elsohaby, I. Molecular Characterization and Antimicrobial Susceptibilities of *Corynebacterium pseudotuberculosis* Isolated from Caseous Lymphadenitis of Smallholder Sheep and Goats, *Animals*, **13** (14), (2023). DOI: 10.3390/ani13142337.

21. World Health Organization. Global antimicrobial resistance and use surveillance system (GLASS) report (2022).

22. Bakr, M., Abdelmalek, S., Suloma, A. and Awad, M. A. Effect of *Aeromonas sobria* Infection on gills and skin histopathology of the Nile tilapia reared under biofloc and clear water systems. *Egyptian Journal of Aquatic Biology and Fisheries*, **25**(5), 933-950 (2021). www.ejabf.journals.ekb.eg.

23. Santos, L. M., Rodrigues, D. M., Alves, B. V. B., Kalil, M. A., Azevedo, V., Barh, D., Meyer, R., Duran, N., Tasic, L. and Portela, R. W. Activity of biogenic silver nanoparticles in planktonic and biofilm-associated *Corynebacterium pseudotuberculosis*, *Peer J.*, **12** e16751 (2024). DOI: 10.7717/peerj.16751.

24. Zhang, P., Gong, J., Jiang, Y., Long, Y., Lei, W., Gao, X. and Guo, D. Application of Silver Nanoparticles in Parasite Treatment. *Pharmaceutics*. **15**(7), 1783, (2023). doi: 10.3390/pharmaceutics15071783.

25. Guimarães, A. de S., Dorneles, E. M. S., Andrade, G. I., Lage, A. P., Miyoshi, A., Azevedo, V., Gouveia, A. M. G., and Heinemann, M. B. Molecular characterization of *Corynebacterium pseudotuberculosis* isolates using ERIC-PCR, *Veterinary Microbiology*, **153** (3–4), 299–306, (2011). DOI: 10.1016/j.vetmic.2011.06.002.

26. Yaman, Ş., Nuhay, Ç., Fındık, A.. and Çiftci, A. Genotyping of *Corynebacterium pseudotuberculosis* isolates using PCR-based DNA fingerprinting methods. *Journal of Microbiological Methods*, **232**, 107122, (2025). DOI: 10.1016/j.mimet.2025.107122.

27. Ruiz-Bolivar, Z., Carrascal-Camacho, A. K., Neuque-Rico, M. C., Gutiérrez-Triviño, C., Rodríguez-Bocanegra, M. X., Poutou-Piñales, R. A. and Mattar, S. Enterobacterial repetitive intergenic consensus-polymerase chain reaction (ERIC-PCR) fingerprinting reveals intra-serotype variations among circulating Listeria monocytogenes strains. *African Journal of Microbiology Research*, **5**(13), 1586-1598, (2011). DOI: 10.5897/ajmr11.033.

28. Sedeik, M. E., El-Shall, N. A., Awad, A. M., Elfeky, S. M., Abd El-Hack, M. E., Hussein, E. O. and Swelum, A. A. Isolation, conventional and molecular characterization of *Salmonella* spp. from newly hatched broiler chicks. *AMB Express*, **9** (1), 136, (2019). DOI: 10.1186/s13568-019-0821-6.

29. Mahmood, Z. K. H., Jesse, F. F., Saharee, A. A., Jasni, S., Yusoff, R. and Wahid, H. Clinio-pathological changes in goats challenged with *Corynebacterium pseudotuberculosis* and its exotoxin (PLD), *American Journal of Animal and Veterinary Sciences*, Science Publications, **10** (3), 112–132, (2015). DOI: 10.3844/ajavsp.2015.112.132.

30. Syame, S. M., Selim, S. A., Ebessy, E. A., Effat, M. M., Hakim, A. S. and Balata, M. A. Evaluation of Protective Efficacy of Mixed PLD Toxoid and Clostridial Vaccines Against Caseous Lymphadenitis (CLA) in Small Ruminants at Egypt, *International Journal of Microbiological Research*, **7** (3), 102–113, (2016). DOI: 10.5829/idosi.ijmr.2016.102.113.

31. Fontaine, M. C., Baird, G., Connor, K. M., Rudge, K., Sales, J. and Donachie, W. Vaccination confers significant protection of sheep against infection with a virulent United Kingdom strain of *Corynebacterium pseudotuberculosis*, *Vaccine*, **24** (33–34), 5986–5996, (2006). DOI: 10.1016/j.vaccine.2006.05.005.

32. Sohier, M. S., Selim, S., Bakry, M., Elgabry, E. and Rehab, M. A. Comparison of protection against caseous lymphadenitis in sheep induced by local isolated strain of *Corynebacterium pseudotuberculosis* by toxoid pld & toxoid pld with Bacterin Vaccine. *International Journal of Development Research*, **7** (9), 15326-15334 (2017). http://www.journalijdr.com.

33. MacFaddin, J. F. *Pruebas bioquímicas para la identificación de bacterias de importancia clínica*. Ed. Médica Panamericana. (2003).

34. European Committee on Antimicrobial Susceptibility Testing (EUCAST). (2024) Breakpoint tables for interpretation of MICs and zone diameters. Version 14.0, valid from 2024-01-01.

35. Magiorakos, A. P., Srinivasan, A., Carey, R. B., Carmeli, Y., Falagas, M. E., Giske, C. G., Harbarth, S., Hindler, J. F., Kahlmeter, G., Olsson-Liljequist, B., Paterson, D. L., Rice, L. B., Stelling, J., Struelens, M. J., Vatopoulos, A., Weber, J. T. and Monnet, D. L. Multidrug-resistant, extensively drug-resistant and pandrug-resistant bacteria: An international expert proposal for interim standard definitions for acquired resistance, *Clinical Microbiology and Infection*, Blackwell Publishing Ltd, **18** (3), 268–281, (2012). DOI: 10.1111/j.1469-0691.2011.03570.x.

36. Sá, M. D. C. A. D., Gouveia, G. V., Krewer, C. D. C., Veschi, J. L. A., Mattos-Guaraldi, A. L. D. and Costa, M. M. D. Distribution of PLD and FagA, B, C, and D genes in *Corynebacterium pseudotuberculosis* isolates from sheep and goats with caseus lymphadenitis. *Genetics and Molecular Biology*, **36**, 265-268, (2013). www.sbg.org.br.

37. Versalovic, J., Koeuth, T. and Lupski, R. Distribution of repetitive DNA sequences in eubacteria and application to fingerprinting of bacterial genomes. *Nucleic Acids Research*, **19**(24), 6823-6831, (1991).

38. Dorneles, E. M. S., Santana, J. A., Ribeiro, D., Dorella, F. A., Guimarães, A. S., Moawad, M. S., Selim, S. A., Garaldi, A. L. M., Miyoshi, A., Ribeiro, M. G., Gouveia, A. M. G., Azevedo, V., Heinemann, M. B. and Lage, A. P. Evaluation of ERIC-PCR as genotyping method for *Corynebacterium pseudotuberculosis* isolates, *PLoS ONE*, , **9**(6), e98758, (2014). DOI: 10.1371/journal.pone.0098758.

39. Heras, J., Domínguez, C., Mata, E., Pascual, V., Lozano, C., Torres, C., & Zarazaga, M. GelJ–a tool for analyzing DNA fingerprint gel images. *BMC Bioinformatics*, **16**(1), 270. (2015). DOI: 10.1186/s12859-015-0703-0.

40. Gomaa, G. Aleid, S.H. EL-Moslamy, A. AlShammari, S. Al-Marshedy, F. Alshammary, J. Gharkan, R. and Abdel-Hameed, E.A. Kamoun, Synergistic efficacy of ZnO quantum dots, Ag NPs, and nitazoxanide composite against multidrug-resistant human pathogens as new trend of revolutionizing antimicrobial treatment, *Discov. Nano*., **19**, 1–22, (2024). https://doi.org/10.1186/S11671-024-04085-7/METRICS.

41. Jenabi, N., Sadeghian, S., Karimzadeh, F., Pour, M. S. and Rakhshan, V. Antibacterial activity and shear bond strength of fiber-reinforced composites and bonding agents containing 0.5%, 1%, 2.5%, and 5% silver nanoparticles. *Dental Research Journal*, **20**(1), 23, (2023).

42. Fernández-Garayzábal, J. F., Collins, M. D., Hutson, R. A., Gonzalez, I., Fernández, E. and Domínguez, L. *Corynebacterium camporealensis* sp. nov., associated with subclinical mastitis in sheep. *International Journal of Systematic and Evolutionary Microbiology*, **48**(2), 463-468, (1998). https://doi.org/10.1099/00207713-48-2-463.

43. Ruiz, H., Ferrer, L. M., Ramos, J. J., Baselga, C., Alzuguren, O., Tejedor, M. T. and Lacasta, D. The relevance of caseous lymphadenitis as a cause of culling in adult sheep. *Animals*, **10**(11), 1962., (2020). https://doi.org/10.3390/ani10111962.

44. Torky, H. A., Saad, H. M., Khaliel, S. A., Kassih, A. T., Sabatier, J. M., Batiha, G. E. S. and De Waard, M. Isolation and molecular characterization of *Corynebacterium pseudotuberculosis*: Association with proinflammatory cytokines in caseous lymphadenitis pyogranulomas. *Animals*, **13**(2), 296, (2023). https://doi.org/10.3390/ani13020296.

45. Borham, M., Oreiby, A., El-Gedawy, A. and Al-Gaabary, M. Caseous Lymphadenitis in Sudanese and Somalian Camels Imported for Meat Consumption in Egypt. *Alexandria Journal of Veterinary Sciences*, **55**(2), 52-59 (2017). DOI: 10.5455/ajvs.282343.

46. Sahu, V., Pathak, M. M., Das, P. and Ravi, A. *Corynebacterium jeikeium* as an Unusual Cause of Keratitis: A Case Report From a Tertiary Care Hospital in Chhattisgarh, India. *Cureus*, **13**(12). (2021). DOI: 10.7759/cureus 20164.

47. Gallardo, A. A., Toledo, R. A., González Pasayo, R. A., Azevedo, V., Robles, C., Paolicchi, F. A. and Estevao Belchior, S. G. *Corynebacterium pseudotuberculosis biovar ovis*: evaluación de la sensibilidad antibiótica in vitro. *Revista argentina de Microbiología*, **51**(4), 334-338,(2019). https://dx.doi.org/10.1016/j.ram.2018.12.001.

48. Li, H., Yang, H., Zhou, Z., Li, X., Yi, W., Xu, Y. and Hu, S. Isolation, antibiotic resistance, virulence traits and phylogenetic analysis of *Corynebacterium pseudotuberculosis* from goats in southwestern China. *Small Ruminant Research*, **168**, 69-75, (2018). https://doi.org/10.1016/j.smallrumres.2018.09.015.

49. Abebe, D. and Sisay Tessema, T. Determination of *Corynebacterium pseudotuberculosis* prevalence and antimicrobial susceptibility pattern of isolates from lymph nodes of sheep and goats at an organic export abattoir, Modjo, Ethiopia. *Letters in Applied Microbiology*, **61**(5), 469-476. (2015). https://doi.org/10.1111/lam.12482.

50. Soriano, F., Zapardiel, J. and Nieto, E. Antimicrobial susceptibilities of *Corynebacterium* species and other non-spore-forming gram-positive bacilli to 18 antimicrobial agents. *Antimicrobial Agents and Chemotherapy*, **39**(1), 208-214. (1995). https://doi.org/10.1128/aac.39.1.208.

51. Rosato, A. E., Lee, B. S. and Nash, K. A. Inducible macrolide resistance in *Corynebacterium jeikeium*. *Antimicrobial Agents and Chemotherapy*, **45**(7), 1982-1989. (2001). https://doi.org/10.1128/aac.45.7.1982-1989.2001.

52. Nagao, P. E., Burkovski, A. and Mattos-Guaraldi, A. L. *Streptococcus* spp. and *Corynebacterium* spp.: Clinical and Zoonotic Epidemiology, Virulence Potential, Antimicrobial Resistance, and Genomic Trends and Approaches. *Frontiers in Microbiology*, **13**, 867210, (2022).

53. Santos, L. M., Stanisic, D., Menezes, U. J., Mendonça, M. A., Barral, T. D., Seyffert, N. and Portela, R. W. Biogenic silver nanoparticles as a post-surgical treatment for *Corynebacterium pseudotuberculosis* infection in small ruminants. *Frontiers in Microbiology*, **10**, 824, (2019).

54. Ramos, C. P., Dorneles, E. M. S., Haas, D. J., Veschi, J. L. A., Loureiro, D., Portela, R. D. and Lage, A. P. Molecular characterization of *Corynebacterium pseudotuberculosis*, *C. silvaticum*, and *C. auriscanis* by ERIC-PCR. *Ciência Rural*, **52**(11), e20210328, (2022).

55. Connor, K. M., Quirie, M. M., Baird, G. and Donachie, W. Characterization of United Kingdom Isolates of *Corynebacterium pseudotuberculosis* Using Pulsed-Field Gel Electrophoresis, *Journal of Clinical Microbiology*, **38**, 7. (2000).

حساسية المضادات الميكروبية والتوصيف الجزيئي لمعزولات بكتيريا كوريني السل الكاذب التي تم عزلها من التهاب الغدد اللمفاوية القيحي في الأغنام

محمد بكر محمد ابراهيم[1]، محمود السيد حشاد[1]، اسلام جمعة وسعد احمد عطية[1]

[1] قسم المكروبيولوجيا، كلية الطب البيطري، جامعة القاهرة، مصر.

[2] مركز أبحاث النانوتكنولوجي (NTRC)، الجامعة البريطانية في مصر، مدينة الشروق، طريق السويس الصحراوي، القاهرة، 11837، مصر

الملخص

تعتبر بكتيريا كوريني السل الكاذب عاملاً مسببًا معروفًا للإصابة بالتهاب الغدد اللمفاوية القيحي (CLA) والتهاب الأوعية اللمفاوية القرحي (UL) في المجترات الصغيرة والكبيرة، على التوالي. يرتبط هذا الممرض في كثير من الأحيان بنتائج علاجية ضعيفة في الحيوانات. في هذه الدراسة، تم تعريف 30 عزلة بكتيرية، تم عزلها من 300 عينة من الغدد اللمفاوية والقيح (10%)، على أنها من نوع الكوريني باكتيريوم. وقد تم التعريف الجزيئي باستخدام PCR للـ 16S rRNA وجين *pld* حيث تم التحقق من 11 من هذه العزلات كنوع بكتيريا كوريني السل الكاذب، بينما تم تحديد عزلة واحدة كنوع بكتيريا كوريني جايكيوم والذي يعتبر اول تسجيل لهذا النوع في الأغنام في مصر. تم إخضاع العزلات لاختبار حساسية المضادات الحيوية والتصنيف الوراثي باستخدام تقنية (ERIC-PCR). صنفت التحليلات العزلات إلى مجموعتين رئيسيتين: المجموعة الأولى (C1) تمثل *C. jeikeium*، والمجموعة الثانية (C2) تمثل *C. pseudotuberculosis*. كما تم تقسيم المجموعة الثانية إلى أربع مجموعات فرعية (2A-2D)، تعكس الروابط الوبائية بين الماشية في محافظتي الجيزة والقاهرة. بالإضافة إلى ذلك، تم تقييم القدرة المضادة للميكروبات لجزيئات الفضة النانوية (AgNPs) وجزيئات الفضة المحملة بالنيتازوكسيد (Ag-NPs/NTZ) ضد كل من *C. pseudotuberculosis* و *C. jeikeium*. وأظهرت النتائج وجود مقاومة متعددة للأدوية (MDR) بين عزلات *C. pseudotuberculosis* و *C. jeikeium* لعدة فئات من المضادات الحيوية. ومع ذلك، أظهرت جميع سلالات *C. pseudotuberculosis* وحساسية 100% للفانكومايسين، والأموكسيسيلين-حمض الكلافيولانيك، والجنتاميسين، والأميكاسين. تدعم هذه النتائج توصية استخدام هذه المستحضرات للتحكم الفعال في CLA. علاوة على ذلك، أظهرت جزيئات الفضة المحملة بالنيتازوكسيد تأثيرًا واعدًا في المختبر ضد كل من أنواع الكورينيبكتيريوم التي تم عزلها في هذه الدراسة وقد تمثل نهجًا مساعدًا محتملاً وجديدًا لمعالجة عدوى *C. pseudotuberculosis*.

الكلمات الدالة: كوريني السل الكاذب، ERIC-PCR، الفضة النانوجزيئية، الفضة النانوجزيئية المحملة على نيتازوكسانيد.